


Investigation of Bubble Contents in Fused Silica Manufactured in an Rotating Plasma Fusion Process Made of Quartz Sand With Different Grades

Rick Augner¹, Robert Danziger^{2,*}, Edda Rädlein¹, and Lars Ortmann²

¹Technische Universität Ilmenau, Germany

²SCHOTT Quartz Glass, Germany

*Correspondence: Robert Danziger, robert.danziger@schott.com

Abstract. The rotational plasma process is a highly efficient method for melting fused silica. Using this method, we prepared glasses with different impurity proportions and examined their bubble contents. The majority of bubbles contained coal gases (type C), while a small proportion contained sulfur gases (type S). Type C bubbles are likely caused by carbon-containing impurities, such as graphite from the electrode. Type S bubbles may be caused by sulfur-containing impurities in the raw material. These results are consistent with those of other authors.

Keywords: Fused Silica, Bubbles, Bubble Content, Mass Spectrometry, Electric Arc, Plasma Fusion

1. Introduction

Silica glass stands out from other glasses because of its “extraordinary properties”, according to Fanderlik [1]. The exceptional thermal properties (low thermal expansion coefficient, high glass transition point), high chemical resistance, and excellent transmission even in the UV range are some of the distinguishing features. As a result, this type of glass is used in a variety of applications, ranging from lamp bodies to the semiconductor industry. [2]

The “electrical rotational plasma melt” is a particularly effective production method. In this process, the granules are placed into a rotating, rotationally symmetrical furnace vessel and held in shape by centrifugal forces. The granules are melted from the inside to the outer layers by a plasma torch that is ignited in the center of the furnace chamber. The melt takes place in the quartz bed as an insulation material. Typically, this process is utilized to create silica glass semi-finished products (crucibles, tubes) that are rotationally symmetrical. Compared to traditional melting, this method has a number of benefits, including low energy loss, a shorter process duration and a reduced risk of contamination by furnace wall materials. [3], [4], [5]

One of the many characteristics of high-quality products is their minimal bubble count. The disadvantage of the previously described method is a rather higher number

of bubbles in the products due to the very short melting time.

According to Pevzner et al. [6], bubbles in silica glass are caused by a variety of factors, including furnace atmosphere, impurities in the raw material, pyrolytic reactions and contamination from the melting furnace. The very low solubility and diffusion of gas species, as well as the slow bubble movement in silica glass, pose significant challenges to possible refining mechanisms.

The use of refining agents as for multicomponent glasses is not possible for high purity fused silica. Bubbles should be avoided in advance. In principle, furnace atmosphere entrapped in the batch, decomposing contaminants and redox reaction are to be considered as bubble sources. The objective of this study was to identify the causes of bubbles in the process of plasma rotation melting. If the causes of bubbles are known, they could potentially be avoided, resulting in fewer bubbles in the material. To this end, silica glasses made from sands with various qualities were melted using the same process parameters. The bubbles created in this way were then compared to each other.

2. Experiments

As part of this study, an investigation was conducted on silica glass tubes obtained through the plasma melting procedure described above. The five glass types (tab. 1) varied in terms of the quantity of bubbles and impurities present, with glass type o1, in contrast to the other glass types, being opaque (fig. 1). The pipes dimensions are displayed in table 2. Quartz sands with varying purity levels were used as raw materials. The glass types o1 and t2 were produced with comparable raw materials.

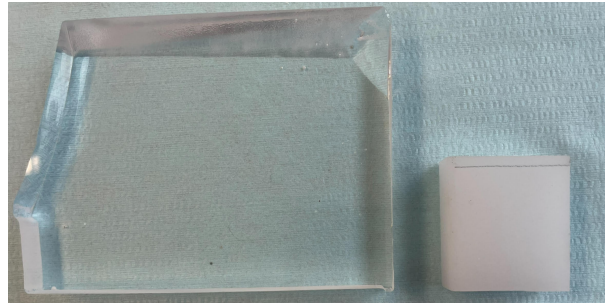


Figure 1. Picture of an transparent glass type sample (t2 - t5) on the left side and opaque glass type sample (o1) right.

Table 1. In the first line the TBCS (Total Bubble Cross Section) value represents the sum of all individual bubble cross-sections in relation to a volume of 100 cm³ [7]. In line 2 – 5 are the maximum impurities (OH; Ca; Fe) of the glasses examined and are given in ppm. The measurements of the impurities were taken by ICP-OES.

Nr.	o1	t2	t3	t4	t5
TBCS [$mm^2 / 100\ cm^3$]	-	7.5	5.5	5.5	1
OH	100	45	45	45	45
Ca	1.5	1.5	1.3	1.1	0.3
Fe	1	1	0.6	0.4	0.3

Table 2. Geometry of the pipes. The minimum and maximum inside and outside diameters are given in [mm]. The pipes, each with a length of 2200 mm, can be divided into four different categories based on their outside diameter ($d_{a_{min}}$). N indicates how many bubbles were examined from each category given in [%].

$d_{a_{min}}$ [mm]	$d_{a_{max}}$ [mm]	$d_{i_{min}}$ [mm]	$d_{i_{max}}$ [mm]	N [%]
505	540	330	428	16.15%
410	495	290	415	49.23%
330	400	190	335	31.54%
227	233	156	175	3.08%

We used as experimental setup a similar procedure as described in Geyer et al. and Ludwig et al. [8], [9]:

The quartz sand was fluidized with argon from a reservoir under low pressure and transferred to a cooled, rotating hollow cylindrical furnace vessel. Vacuum was created. Following the filling of the furnace vessel, an electric arc was ignited in the center as a heat source to melt the glass from the inside to the outside in the raw material's own bed (fig. 2). We used argon, hydrogen and nitrogen as operating gases of the electric arc. When the heating power no longer exceeded the cooling power applied from the outside, the melting process was terminated. The melt was performed as a vacuum compression melt with two pressure stages: In phase 1, melting, the melt was under low pressure (minimum 0.2 bar). In phase 2, homogenization, high pressure (maximum 10 bar) was applied. Notably, glass type o1 did not undergo a low pressure phase and the melting was performed during the high pressure (2). The entire generation process took no more than two hours to complete. Subsequently, the tubes produced through this manufacturing method underwent stress-free annealing at approximately 1100 °C. For this annealing a second furnace was used which operated with air. The process parameters are shown in table 3. [10]

Table 3. Melting parameters of the silica glass tubes.

filling gases	Ar; N ₂ ; O ₂
operating gases	Ar; N ₂ ; H ₂
p_{min} [bar]	0.2
p_{max} [bar]	10.0
t_{max} [min]	120.0
T_{max} [° C]	2200.0

Bubbles present in the silica glass tubes were primarily cut out of the sample body in the radial center, subjected to microscopic examination, and analyzed to determine their gas composition. The gas content analysis was performed using the bubble content analyzer inProcess Instruments GIA 522. The bubbles were prepared out of the glass sample and then broken in the evacuated measuring chamber of the device under ultra-high vacuum using a breaking needle. The released bubble contents were measured using the dynamic measurement principle according to Koprio [11]. Each type of glass underwent at least ten bubble content analyses. The bubbles from types t2 – t5 had a diameter of 100 – 300 μm .

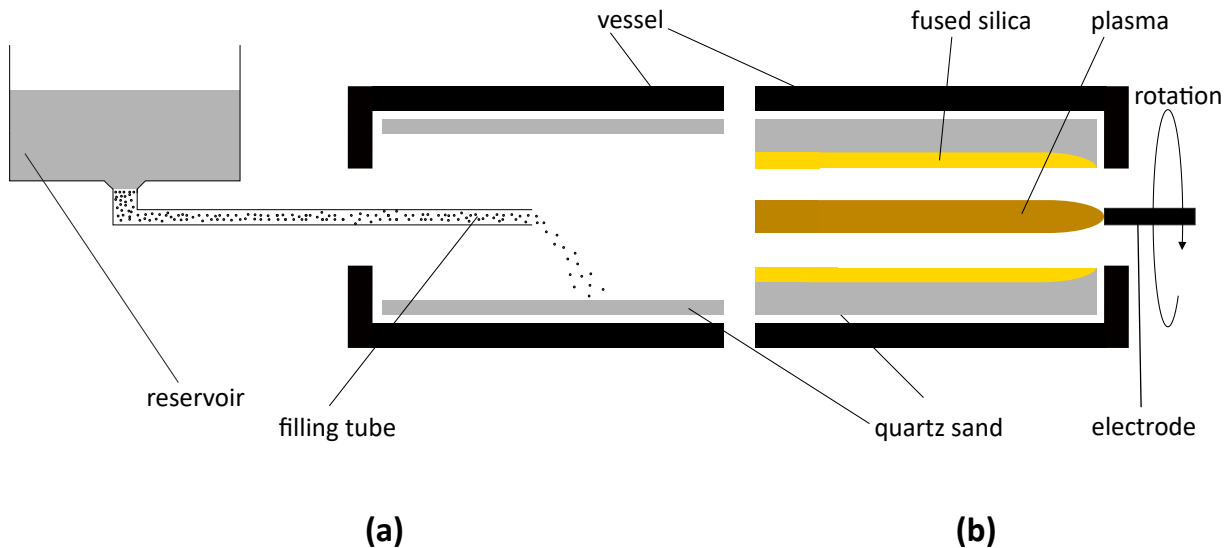


Figure 2. Schematic of a tubular electrical rotational plasma melt: a) shows the filling of the rotating furnace vessel from a reservoir and b) the subsequent melting of the hollow silica glass cylinder: the granulate, held in shape by centrifugal force, is melted from the inside to the outside in its own bed of quartz sand by a centrally ignited electric arc ("plasma").

3. Results and Discussion

Fig. 3 and tab. 5 show the measurement results of all measured bubbles of glass types o1 – t5, each as an average value. It was found that the bubbles in o1 consisted mainly of Ar and contained small amounts of H₂; N₂ and O₂ (fig. 3). Due to the filling technology argon and minimal amounts of air (nitrogen, oxygen) could be entrapped in the interstices of the sand fill and were unable to be evacuated during the process. The hydrogen we found could have originated from the electric arc, where hydrogen is one of the operating gases (tab. 3). The interstitial gases found in the sand fill were thus stabilized as bubbles. This aligns well with Pevzner et al. [6]

The bubbles observed in transparent glass types t2 to t5 could be categorized into two distinct types: Type C bubbles consisted mainly of carbon gases (CO; CO₂, fig. 4) and type S bubbles of sulfur gases (COS; H₂S; SO₂, fig. 5). The bubbles contain not only the main components, but also Ar, H₂ and N₂. These gases are, similar to the results of o1, most likely due to atmosphere entrapped in the interstices of the sand fill. The type C were found in the full range of 100 – 300 μm , while type S bubbles were mostly around 100 – 130 μm in size.

With the exception of the precise ratios of gases within the bubble, the type C bubble composition stayed consistent and consisted primarily of a mixture of CO and CO₂ with smaller proportions of Ar, N₂ and H₂ (fig. 4). The exact composition of the bubbles was independent of the impurity level. The carbon gas contents are likely due to CO_x-releasing impurities. We suspect a common cause since these bubbles were found in all transparent glass types (t2 to t5). According to Paulsen et al. [12], these bubbles may be caused by graphite from the electrodes. Organic impurities in the raw material are an additional possibility. The carbon sources may undergo pyrolysis as a result of the reducing atmosphere, or they may be oxidized by the SiO₂ (eqs. 1; 4). There is still much to learn about the reaction mechanisms. The notable CO content observed in the type C bubbles (fig. 4) appears to require a carbon source, either from electrodes or organic impurities. If contaminating carbonates would break down, they would release CO₂. This would need to be transformed into CO by the Boudouard

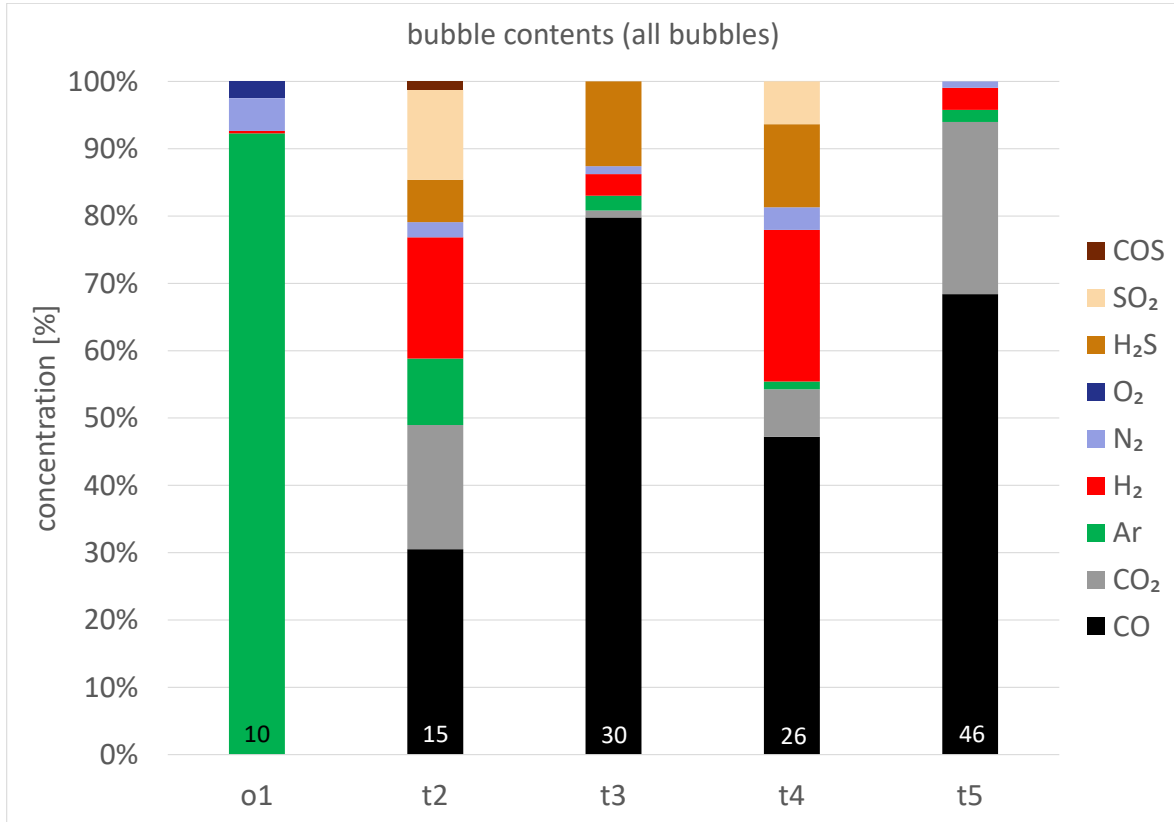
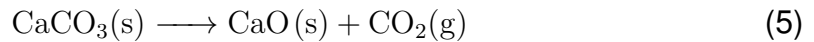
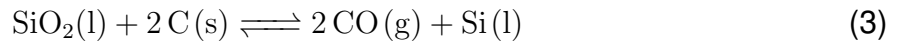
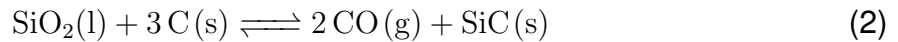
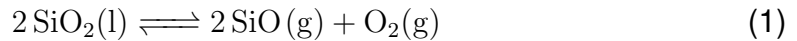


Figure 3. Bubble contents of all bubbles of glass types o1 – t5, each as an average value. Since the o1 was a opaque material we couldn't investigate single bubbles. The bubbles of the transparent materials t2 – t5 had a diameter of 100 – 300 μm . The number of investigated samples per material is given by the number at the bottom of the diagram.

equilibrium (eqs. 5 – 6) if the proportion of CO does not directly originate from carbon-containing impurities. [13]

Type C bubbles partially showed black adhesions on the inner edge of the bubble (fig. 6a) [14]. Thus, the internal adhesions observed are presumed to be carbon containing deposits, which could be resublimated due to the Boudouard equilibrium (eq. 6). This would support the thesis of the presence of carbon as a source of CO by oxidation or by the transformation of CO₂ due to the Boudouard equilibrium. However, since the SiO₂ melt itself tends to decompose at high temperatures, it is also possible that deposits consist of SiC or Si, which are resublimated during cooling (eqs. 1 - 3).



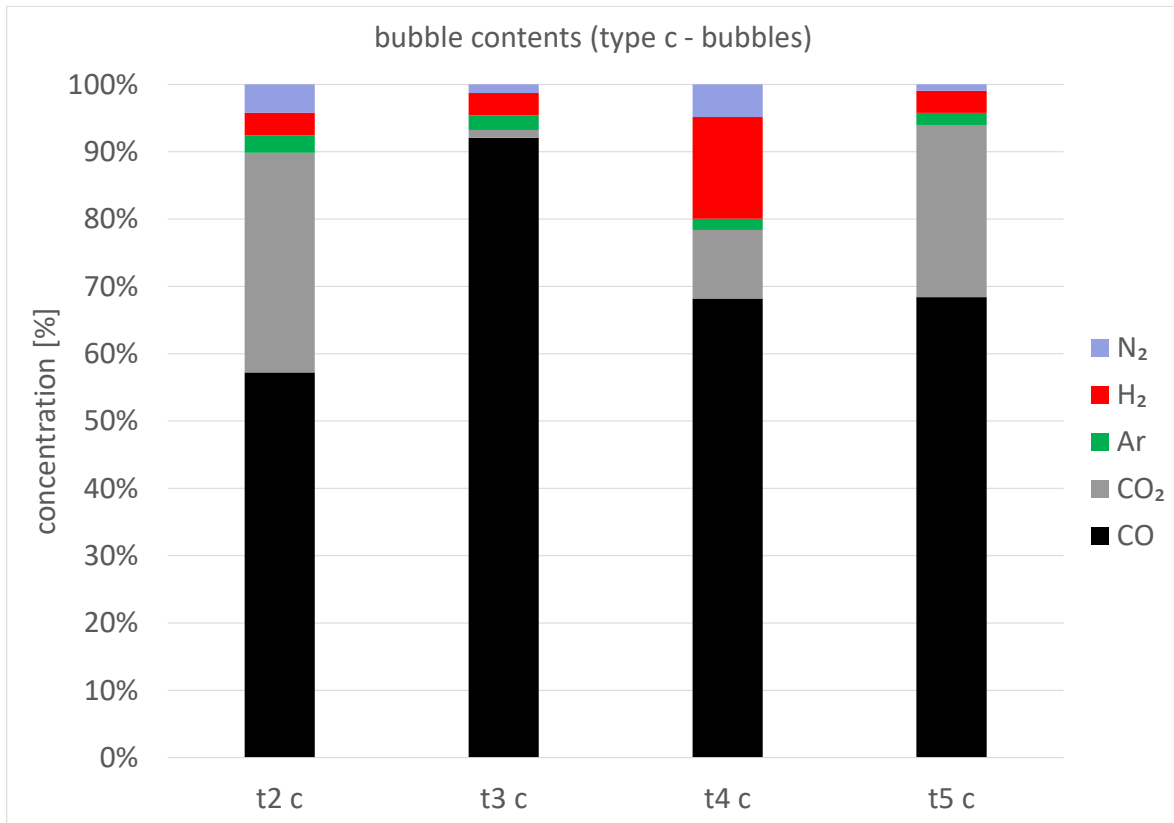


Figure 4. Bubble contents of type C bubbles of glass types t2 – t5, each as an average value. Glass type o1 isn't shown since we didn't found type C bubbles in this glass type.

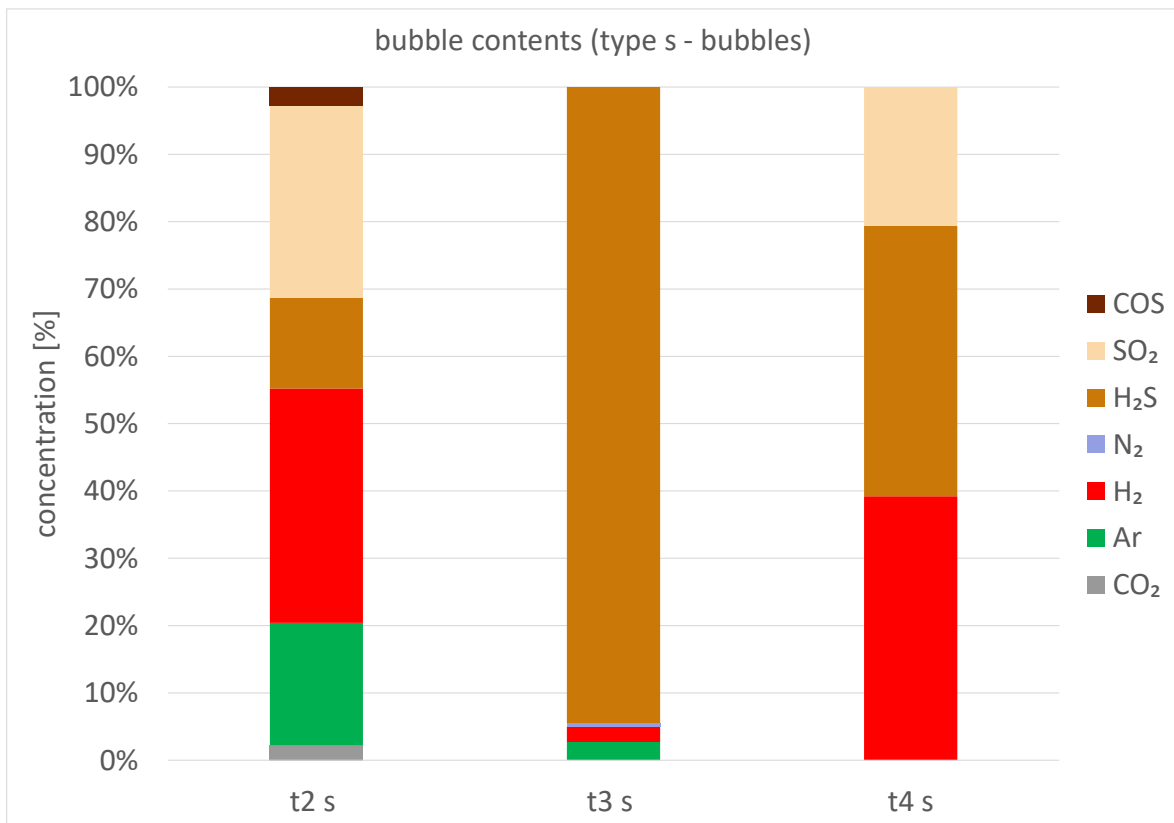


Figure 5. Bubble contents of type S bubbles of glass types t2 – t4, each as an average value. Glass type o1 and t5 aren't shown since we didn't found type S bubbles in these glass types.

Bubbles of type S were exclusively identified in samples t2 to t4, which had a significantly higher content of impurities, compared to sample t5. Their abundance was notably lower compared to bubbles of type C (tab. 4). Brown streaks were occasionally observed in the glass right next to these bubbles (fig. 6b – 6c). The gases found were mostly sulfur-containing (COS , H_2S , SO_2) and H_2 . In certain cases, the composition of the individual bubbles varied significantly. As an illustration, while some bubbles displayed only H_2S , others displayed a combination of mostly H_2 and a lower amount of H_2S . In isolated bubbles, traces of Ar and CO_2 were discovered.

The brown impurities near the bubbles might originate from an iron – sulfur compound (FeS ; FeS_2 ; ...). These compounds might be found as impurities in the granules. If an interstices of the sand fill is formed to a bubble through the melt, an impurity could be near to this bubble and get in contact to the entrapped gases. There, it might be converted with the entrapped gases to form iron and sulfur-containing gas (eqs. 7; 8). The reactants necessary for the formation of the iron-sulfur compound were likely provided by the filling and operating atmosphere (tab. 3), specifically H_2 and O_2 . The small amount of reactants provided by the Fe_xS_y – impurities might be the reason for the smaller average bubble size (100 – 130 μm) of this bubble type. Therefore, using higher quality raw materials with smaller amounts of iron impurities may reduce or eliminate type S bubbles. [15]

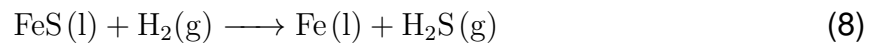
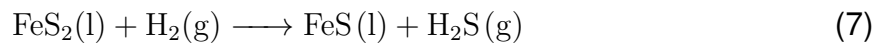


Table 4. distribution of type S and type C-bubbles in different samples

sample	type C	type S
t2	53 %	47 %
t3	87 %	13 %
t4	63 %	37 %
t5	100 %	0 %

Table 5. Bubble contents of all bubbles of glass types o1 – t5, each as an average value. Since the o1 was a opaque material we couldn't investigate single bubbles. The bubbles of the transparent materials t2 – t5 had a diameter of 100 – 300 μm . Since the o1 was a opaque material we couldn't investigate single bubbles. The uncertainties are given in the σ -rows.

	Ar	σ Ar	H ₂	σ H ₂	N ₂	σ N ₂	O ₂	σ O ₂	CO	σ CO	CO ₂	σ CO ₂	H ₂ S	σ H ₂ S	SO ₂	σ SO ₂	COS	σ COS
o1	92%	0,1%	0,4%	0%	4,9%	0,1%	2,5%	0,1%	0%	0%	0%	0%	0%	0%	0%	0%	0%	0%
t2	9,9%	0,7%	18%	1,4%	2,2%	0,7%	0%	0%	31%	0,8%	18%	0,8%	6,3%	0,1%	13%	0,5%	1,3%	0,2%
t2 c	2,6%	0,1%	3,3%	0,8%	4,2%	1,3%	0%	0%	57%	1,5%	33%	1,1%	0%	0%	0%	0%	0%	0%
t2 s	18%	1,3%	35%	2,1%	0%	0%	0%	0%	0%	0%	2,3%	0,5%	13%	0,2%	29%	1,1%	2,8%	0,5%
t3	2,2%	0,2%	3,2%	1,0%	1,2%	0,5%	0%	0%	80%	1,2%	1,0%	0,1%	13%	0,1%	0%	0%	0%	0%
t3 c	2,1%	0,2%	3,4%	1,0%	1,3%	0,5%	0%	0%	92%	1,4%	1,2%	0,2%	0%	0%	0%	0%	0%	0%
t3 s	2,7%	0,2%	2,3%	0,7%	0,5%	0,1%	0%	0%	0%	0%	0,0%	0,0%	94%	0,6%	0%	0%	0%	0%
t4	1,2%	0,1%	23%	1,7%	3,3%	0,4%	0%	0%	47%	1,1%	7,0%	0,6%	12%	0,2%	6,4%	0,2%	0,0%	0,0%
t4 c	1,6%	0,2%	20%	1,8%	4,6%	0,5%	0%	0%	65%	1,6%	9,6%	0,9%	0,0%	0%	0%	0%	0%	0%
t4 s	0%	0%	31%	1,5%	0%	0%	0%	0%	0%	0%	0,0%	0,0%	46%	0,6%	24%	0,9%	0,0%	0%
t5	1,7%	0%	3,3%	0,2%	0,9%	0%	0%	0%	68%	0,3%	26%	0,1%	0%	0%	0%	0%	0%	0%

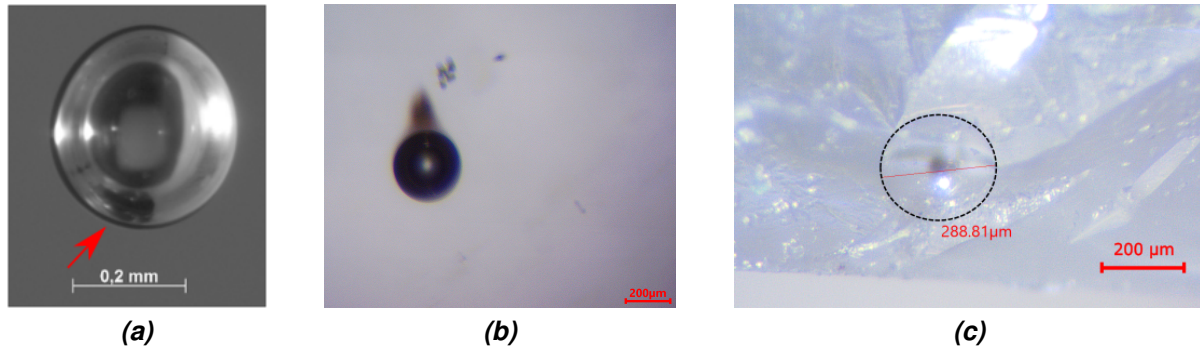


Figure 6. (a) Black inclusion at the edge of a closed type-C-bubble. [14] (b) Brownish inclusion near to a closed type-S-bubble. (c) Brownish inclusion in the middle of an opened type-S-bubble (the black ring marks the edge of the opened bubble).

4. Conclusion

In the present work, we investigated the bubble contents in silica glasses of various qualities that were manufactured by a tubular, electrical rotational plasma melt. Two distinct types of bubbles were identified: Type C bubbles, predominantly composed of carbon gases, and type S bubbles, primarily containing sulfur-containing gases and hydrogen. Type C bubbles were present in all transparent glasses, indicating a potential shared cause. We found no correlation between the level of impurities and the composition of the type C bubbles. Paulsen et al. [12] suggest the involvement of carbon from the electrodes, while another possibility is the consideration of (organic) impurities within the sand. These impurities could undergo oxidation or pyrolytic decomposition, and the precise reaction mechanisms should be the focus of future investigations.

The absence of type S bubbles in the highest quality sample t5 (tab. 4) and their occasional association with brown impurities (fig. 6b to 6c) lead us to suspect that these bubbles might be induced by iron-sulfur-containing impurities present in the raw material. It is conceivable that these impurities could react with H_2 or O_2 , resulting in the formation of sulfur gases observed in the bubbles. Using higher quality raw materials may reduce or eliminate type S bubbles. However, the confirmation of iron compounds in the brown inclusions is still pending.

Data availability statement

The data that support the findings of this study are proprietary and confidential in nature, as they contain sensitive business information. Therefore, they are not publicly available. Access to these data may be granted on a case-by-case basis, subject to the approval of QSIL GmbH Quarzschmelze Ilmenau. For inquiries regarding data access, please contact Robert Danziger at robert.danziger@schott.com.

Author contributions

RA: investigation, visualisation, Formal analysis, writing – original draft, writing – review & editing; **RD:** investigation, visualisation, Formal analysis, writing – review & editing; **ER:** supervision, conceptualisation, writing – review & editing; **LO:** supervision, conceptualisation, writing – review & editing

Competing interests

The authors declare that they have no competing interests.

Acknowledgements

We would like to thank the team of Ralph Seuwen from Schott AG for their assistance in capturing the microscopy images and helpful discussions. We also acknowledge the valuable input and support of our colleagues Frank-Peter Ludwig, Felix Schröckert and Robert Hahn during the course of this research.

References

- [1] "Significance and classification of silica glasses," in *Silica glass and its application*, ser. Glass science and technology, I. Fanderlik, Ed., vol. 11, Amsterdam and New York: Elsevier, 1991, pp. 15–16, ISBN: 9781483291680.
- [2] R. S. Nasyrov and V. M. Lopatin, "Vacuum Melting of Quartz Glass with Layered Filling of a Crucible," *Glass and Ceramics*, vol. 74, no. 3-4, pp. 115–117, 2017, ISSN: 0361-7610. DOI: [10.1007/s10717-017-9941-0](https://doi.org/10.1007/s10717-017-9941-0).
- [3] A. Kröner, *Verfahren zum Herstellen von Rohren oder anderen Hohlkörpern aus Quarz und anderen schwer schmelzbaren Stoffen*, German, DE543957C, Applicants: W.C. Heraeus G.m.b.H., 1932. [Online]. Available: <https://depatisnet.dpma.de/DepatisNet/depatisnet?action=bibdat&docid=DE000000543957A>.
- [4] W. Reiss, "Entwicklung von Rotationsplasmaöfen zum Kieselglasschmelzen," German, *Elektrowärme international. Edition B, Industrielle Elektrowärme*, vol. 49, no. 2, B93–B98, 1991.
- [5] G. K. Warden, M. Juel, B. A. Gawel, and M. Di Sabatino, "Recent developments on manufacturing and characterization of fused quartz crucibles for monocrystalline silicon for photovoltaic applications," *Open Ceramics*, vol. 13, p. 100321, 2023, ISSN: 26665395. DOI: [10.1016/j.oceram.2022.100321](https://doi.org/10.1016/j.oceram.2022.100321).
- [6] B. Z. Pevzner and S. V. Tarakanov, "Bubbles in Silica Melts: Formation, Evolution, and Methods of Removal," in *Glass: Selected Properties and Crystallization*, J. W. P. Schmelzer, Ed., Berlin: De Gruyter, 2014, pp. 301–376, ISBN: 9783110298581. DOI: [10.1515/9783110298581](https://doi.org/10.1515/9783110298581).
- [7] *Optisches Glas; Technische Lieferbedingungen*, German, DIN 58927:1970-2, Berlin, 1970. [Online]. Available: <https://www.dinmedia.de/de/norm/din-58927/741779>.
- [8] H. Geyer, E. Kathe, T. Kreuzberger, and B. Schwieger, *Verfahren zur Herstellung von rotationssymmetrischen Kieselglashohlkörpern*, German, DD300972A7, Applicants: Ilmenauer Glaswerk GmbH, 1992. [Online]. Available: <https://depatisnet.dpma.de/DepatisNet/depatisnet?action=bibdat&docid=DD300972A7>.
- [9] F.-P. Ludwig, L. Ortmann, J. Wehner, and R. Heubach, *Hohlzylinder aus keramischem Material, ein Verfahren zu seiner Herstellung und seine Verwendung*, German, DE102016118826A1, Applicants: QSIL GmbH Quarzschmelze Ilmenau, 2016. [Online]. Available: <https://depatisnet.dpma.de/DepatisNet/depatisnet?action=bibdat&docid=DE102016118826A1>.
- [10] "The technology of silica glass manufacture," in *Silica glass and its application*, ser. Glass science and technology, I. Fanderlik, Ed., vol. 11, Amsterdam and New York: Elsevier, 1991, pp. 95–193, ISBN: 9781483291680.
- [11] J. A. Koprio, H. Gaug, and H. Eppler, "Analysis of small gas volumes: Inclusions in glass, gas filled lamps and sealed semiconductor packages," *International Journal of Mass Spectrometry and Ion Physics*, vol. 48, pp. 23–26, 1983, ISSN: 00207381. DOI: [10.1016/0020-7381\(83\)87019-3](https://doi.org/10.1016/0020-7381(83)87019-3).

- [12] O. Paulsen, S. Rørvik, A. M. Muggerud, and M. Juel, “Bubble distribution in fused quartz crucibles studied by micro X-Ray computational tomography. Comparing 2D and 3D analysis,” *Journal of Crystal Growth*, vol. 520, pp. 96–104, 2019, ISSN: 00220248. DOI: [10.1016/j.jcrysgro.2019.05.002](https://doi.org/10.1016/j.jcrysgro.2019.05.002).
- [13] P. Lahijani, Z. A. Zainal, M. Mohammadi, and A. R. Mohamed, “Conversion of the greenhouse gas CO₂ to the fuel gas CO via the Boudouard reaction: A review,” *Renewable and Sustainable Energy Reviews*, vol. 41, pp. 615–632, 2015, ISSN: 13640321. DOI: [10.1016/j.rser.2014.08.034](https://doi.org/10.1016/j.rser.2014.08.034).
- [14] R. Seuwen, L. Dohmen, and S. Krause, “Blaseninhaltsveränderung in Blasen in Kieselglas,” German, Schott AG, internal report for QSIL GmbH, 2020.
- [15] H. Mulfinger, “Gase (Blasen) in der Glasschmelze,” German, in *Glastechnische Fabrikationsfehler*, H. Jebsen-Marwedel and R. Brückner, Eds., Berlin, Heidelberg: Springer Berlin Heidelberg, 2011, ISBN: 978-3-642-16432-3. DOI: [10.1007/978-3-642-16433-0](https://doi.org/10.1007/978-3-642-16433-0).